Check for updates

Decoding the infrared spectra changes upon formation of molecular complexes: the case of halogen bonding in pyridine···perfluorohaloarene complexes†

Alex Iglesias-Reguant, [ab] Heribert Reis,[c] Miroslav Medveď',[de] Borys Ośmiałowski, [a] Robert Zaleśny [*f] and Josep M. Luis [*b]

A recently developed computational scheme is employed to interpret changes in the infrared spectra of halogen-bonded systems in terms of intermolecular interaction energy components (electrostatic, exchange, induction, dispersion) taking pyridine···perfluorohaloarene complexes as examples. For all complexes, we find a strong linear correlation between the different terms of the interaction-induced changes of the IR band associated with an intermolecular halogen bond stretching mode and the corresponding terms of the interaction energy, which implies that the interaction components play similar roles in both properties. This is not true for other vibrational modes localized in one of the monomers studied here, for which the corresponding interaction-induced changes in IR bands may present a completely different decomposition than the interaction energy.

Intermolecular interactions have a key role in the physicochemical properties of matter, such as solubility, reactivity, or all types of spectroscopic signatures, to name a few. Over the last decades, several theoretical frameworks have been developed to analyze the effect of the different intermolecular forces on the properties of the matter,[1–10] allowing the understanding of their fundamental aspects in a plethora of molecular systems

covering a wide palette of interaction types and strengths. Nowadays the methodology to analyze intermolecular interactions is an important part of modern interpretive chemistry and it is used to understand the physical origin of the experimental manifestations of intermolecular interactions. Myriads of atomic and molecular complexes have been studied using energy decomposition analyses, thus enriching the rationalization of the basic interaction types that govern the structure, stability, and properties of molecular complexes and their organization at larger scales.

Spectroscopic techniques, with infrared (IR) spectroscopy at the forefront, are frequently used to substantiate the formation of molecular complexes. The popularity of IR spectroscopy is due to its high interpretive power, *e.g.*, the presence of hydrogen bonds in molecular complexes can be identified easily by the change of the frequency of the bands associated with the vibrational modes of functional groups involved in the intermolecular interaction,[11,12] a feature listed by IUPAC[13] as a criterion to call the interaction hydrogen bond (similar applies for halogen bonds).[14] Spectroscopic IR studies are often paralleled by computational efforts in the framework of the theory of intermolecular interactions to link the strength of the interactions with specific interaction types (exchange, electrostatic, induction, dispersion).[15,16] However, none of the performed studies attempted to analyze the changes in the intensity and frequency of the peaks of IR spectra in terms of interaction types since the available decomposition schemes were primarily developed for interaction energies. To overcome this limitation, we recently developed a new scheme to interpret the nature of the changes in infrared spectra occurring upon the formation of a molecular complex.[17] This new scheme, called infrared spectra decomposition analysis (IRS-DA) allows the association of the simultaneous changes in the intensity and frequency of each peak of the IR spectra occurring upon complex formation with the different interaction types (*i.e.* exchange, electrostatic, induction, dispersion). Specifically, IRS-DA decomposes the changes in the ratio between intensity

a Faculty of Chemistry, Nicolaus Copernicus University, Gagarina 7,
PL-87100 Toruń, Poland

b Institute of Computational Chemistry and Catalysis and Department of Chemistry,
University of Girona, Campus de Montilivi, 17003, Girona, Catalonia, Spain.
E-mail: josepm.luis@udg.edu

c Institute of Chemical Biology, National Hellenic Research Foundation (NHRF),
Vassileos Constantinou Ave 48th, 116 35 Athens, Greece

d Department of Chemistry, Faculty of Natural Sciences, Matej Bel University,
Tajovského 40, SK-97400 Banská Bystrica, Slovak Republic

e Regional Centre of Advanced Technologies and Materials,
Czech Advanced Technology and Research Institute (CATRIN),
Palacký University in Olomouc, Šlechtitelu 27, 783 71 Olomouc, Czech Republic

f Faculty of Chemistry, Wroclaw University of Science and Technology,
Wybrzeże Wyspiańskiego 27, 50-370 Wrocław, Poland.
E-mail: robert.zalesny@pwr.edu.pl

† Electronic supplementary information (ESI) available. See DOI: https://doi.org/10.1039/d3cp02412a

This journal is © the Owner Societies 2023

Phys. Chem. Chem. Phys., 2023, **25**, 20173–20177 | **20173**

and frequency squared for each normal mode upon **AB** complex formation from monomers **A** and **B**. IRS-DA provides information regarding the interplay of interaction types, i (exchange, electrostatic, induction, dispersion), and their manifestation through changes in the band position and intensity of normal mode a:

$$\Delta\left(\frac{I_a^i}{\omega_a^{2,i}}\right) = \frac{I_a^i}{\omega_a^{2,i}}(\mathbf{AB}) - \frac{I_a^i}{\omega_a^{2,i}}(\mathbf{A}) - \frac{I_a^i}{\omega_a^{2,i}}(\mathbf{B}) \quad (1)$$

Note that for bands that undergo negligible frequency changes upon complex formation, or for which $\frac{I_a^i}{\omega_a^{2,i}}(\mathbf{A}) = \frac{I_a^i}{\omega_a^{2,i}}(\mathbf{B}) = 0$, the above equation can be simplified to:

$$\Delta I_a^i = I_a^i(\mathbf{AB}) - I_a^i(\mathbf{A}) - I_a^i(\mathbf{B}) \quad (2)$$

thus allowing for direct decomposition of ΔI_a into interaction types i. The net change in IR intensity for mode a (ΔI_a) can be expressed as the sum of all considered interaction types i.

In this communication, we report the first analysis of IR intensity changes upon the formation of halogen-bonded (XB) complexes, using the molecular complexes formed by pyridine (**pyr**) and perfluorohaloarenes (C_6F_5X, where X is Cl, Br, or I) as examples (Fig. 1). As demonstrated in our previous work, halogen bond formation in complexes containing pyridine can be identified using spectroscopic techniques, including IR spectroscopy.[18] In particular, the measured IR spectrum of a 1:1 mixture of pyridine and C_6F_5I featured a new band at 195 cm^{-1} not present in the IR spectra of the pure liquids pyridine or C_6F_5I. This new band was assigned to the intermolecular C–I···N stretching, in agreement with the theoretical IR spectra obtained at the MN15/aug-cc-pVDZ(PP) level[18] and previous measurements for the cocrystal.[19] Thanks to the newly developed IRS-DA method it is now possible to link the formation of this band with individual intermolecular interaction types.[17] XB complexes are nowadays in the limelight due to the unique properties of halogen bonding and its wide range of applications,[20] such as in crystal engineering[21] of emissive materials,[22,23] sensing enhancement[24] or in medicine.[25–27] The term halogen bond is applied to a directional intermolecular interaction involving an electrophilic region (so-called σ-hole) associated with a halogen atom and a nucleophilic second atom. The σ-hole was described theoretically already a

long time ago,[28] and has been invoked as an explanation for many phenomena. However, it was only very recently possible to visualize the σ-hole directly by Kelvin probe force microscopy.[29] Halogen bonding resembles hydrogen bonding (HB) in many aspects, including, in strongly interacting molecules, intermolecular migration of the heavy halogen atom, similar to proton transfer in certain hydrogen-bonded complexes.[30] Given the widespread interest in XB complexes and their possible coexistence with hydrogen bonding, as exemplified in supramolecular synthons,[31] we consider the analysis of changes in spectroscopic vibrational signatures in terms of interaction types very timely. Intermolecular interactions influence the location and topology of the potential energy minima and the electron density distribution of the molecules that form the complexes, which in turn affects both the position and the intensity of the bands in the IR spectra.

In order to perform the analysis of ΔI_a upon complex formation in terms of interaction types i we choose the general framework of decomposition of the interaction energy at the second-order Møller–Plesset perturbation theory (MP2) level based on the variational-perturbational decomposition scheme (VP-EDS).[32–36] According to VP-EDS, the total interaction energy of a dimer is partitioned into several interaction energy terms as defined in the symmetry-adapted perturbation theory (SAPT).[32–35] At the MP2 level, the total VP-EDS interaction energy of the complex calculated by a supermolecular approach in the dimer-centered-basis set (DCBS)[37] is partitioned into the Hartree–Fock (HF) (ΔE_{int}^{HF}) and the electron correlation interaction energy correction (ΔE_{corr}^{MP2}):

$$\Delta E_{int}^{MP2} = \underbrace{\varepsilon_{el}^{(10)} + \Delta E_{ex}^{HL} + \Delta E_{del}^{HF}}_{\Delta E_{int}^{HF}} + \underbrace{\varepsilon_{el,r}^{(12)} + \varepsilon_{disp}^{(20)} + \Delta E_{ex}^{(2)}}_{\Delta E_{corr}^{MP2}} \quad (3)$$

The HF term encompasses the electrostatic interactions of the charge densities of the unperturbed subsystems, $\varepsilon_{el}^{(10)}$, the exchange repulsion (ΔE_{ex}^{HL}), and the charge delocalization (ΔE_{del}^{HF}). The last two terms account for exchange effects due to the Pauli antisymmetry principle and induction, respectively. The second-order electron correlation term includes the electron correlation correction to the first-order electrostatic interaction, $\varepsilon_{el,r}^{(12)}$, the second-order dispersion interaction, $\varepsilon_{disp}^{(20)}$, and the remaining second-order electron correlation effects ($\Delta E_{ex}^{(2)}$).[34,36,38]

We will start the analysis of the **pyr**:C_6F_5X complexes with the partitioning of the intermolecular interaction energy (ΔE). Fig. 2a and Table S1 (ESI†) show the MP2 interaction energies and their components for the three complexes ordered according to the increasing value of the total interaction energy. As expected, the absolute value of the VP-EDS/MP2 interaction energy is largest for the complex containing iodine, and it decreases with increasing electronegativity (χ) of atom X, (i.e., $\Delta E(I) > \Delta E(Br) > \Delta E(Cl)$). The partitioning of the interaction energy for the three **pyr**:C_6F_5X complexes reveals a large destabilizing exchange-repulsion contribution, which is canceled by the sum of the electrostatic and delocalization terms, thus predicting only very weak binding at the uncorrelated level
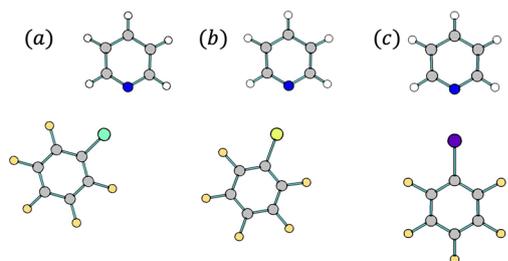

Fig. 1 Optimized structures of the studied halogen-bonded complexes, composed of pyridine and (a) C_6F_5Cl, (b) C_6F_5Br or (c) C_6F_5I.

20174 | *Phys. Chem. Chem. Phys.*, 2023, **25**, 20173–20177

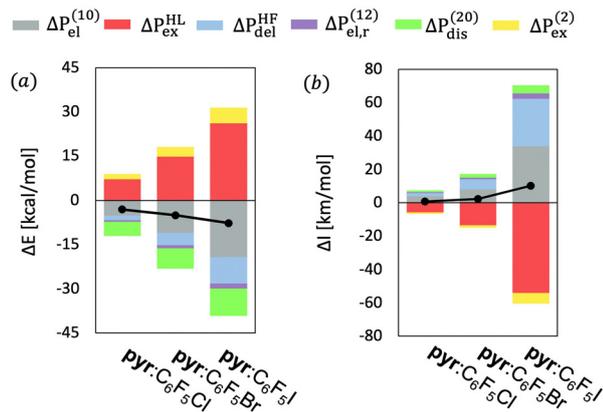This journal is © the Owner Societies 2023

Fig. 2 Partitioning of (a) the interaction energy ($\Delta P = \Delta E$) and (b) the excess IR intensity ($\Delta P = \Delta I$) of the intermolecular vibrational stretching mode (ν_a^{int}) for the **pyr**:C_6F_5X complexes at the equilibrium geometries at the MP2/aug-cc-pVDZ-PP level of theory. The black dots combined with black lines indicate the total excess properties.

Fig. 3 Difference IR spectrum obtained by subtracting the simulated IR spectra of pyridine and C_6F_5I from the IR spectrum of **pyr**:C_6F_5I complex, as well as the displacements of: (a) an intermolecular vibrational stretching mode (ν_a^{int}), (b) a C–X stretching mode of C_6F_5I, which involves a change in the halogen bond distance (ν_b^{C-X}), (c) one local vibrational mode of C_6F_5I ($\nu_c^{C_6F_5I}$) and (d) one local vibrational mode of pyridine (ν_c^{pyr}).

(Table S1, ESI†). Thus, the observed stability of the studied complexes is mostly due to the sum of the electron correlation terms, especially $\Delta\varepsilon_{disp}^{(20)}$ and $\Delta E_{ex}^{(2)}$, to the total interaction energies.

Fig. 2a shows that the interplay of the interaction energy components for the three **pyr**:C_6F_5X complexes is very similar, *i.e.* the relative weight of the different interaction terms contributing to ΔE for the three different halogen bonds resembles each other to a large extent (see also Fig. S1, ESI†). We may thus conclude that the stability of these different XB complexes with the nitrogen atom in pyridine as the nucleophilic partner has a similar physical origin, in the sense that the different elements of the intermolecular interaction lead to comparable relative contributions to the total excess energy. We note that a similar conclusion can be drawn from the good linear fits with negligible y-intercept between the ΔE and ΔE^i terms of **D**:C_6F_5X (where **D** represents a fluoroborate-based dye containing pyridine, see Fig. S2, ESI†)[18] and the corresponding terms of **pyr**:C_6F_5I, as shown in Fig. S3 and Table S2 (ESI†).

Furthermore, the partition of ΔE for these six complexes follows the same trends observed in previous studies of small halogen-bonded dimers performed by our group, indicating that the nature of halogen bonding is similar for complexes of different chemical composition.[39] Table S3 (ESI†) presents the R^2 of the linear fits between partition terms of the intermolecular interaction energy of all the XB and HB complexes studied in this work and three complexes in π–π stacking arrangement studied in the ref. 17 The complexes presenting the same type of non-covalent interaction share a very similar physical origin (*i.e.*, $R^2 > 0.89$). On the contrary, this is not true for systems that present different types of non-covalent interactions (*i.e.*, R^2 as low as 0.39).

The difference IR spectrum of **pyr**:C_6F_5I displayed in Fig. 3 reveals significant changes in the IR spectra of the individual constituents upon complexation. Our IRS-DA analysis will be focussed on four representative bands attributed to (a) the intermolecular vibrational stretching mode (ν_a^{int}); (b) the C–I
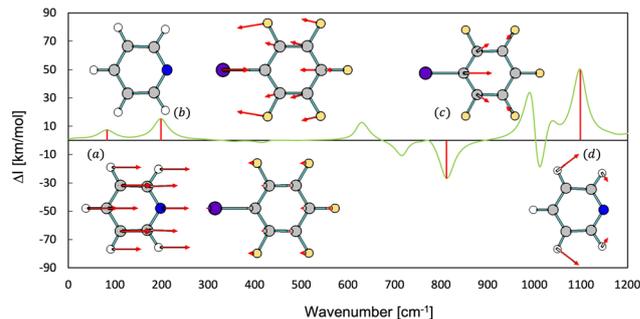
stretching, which implies a change in the halogen bond distance (ν_b^{C-X}); and two vibrational modes that involve movements of the atoms of only one monomer: (c) a distortion of the ring of the C_6F_5 I, ($\nu_c^{C_6F_5I}$) and (d) a rocking in-plane bending of the hydrogens of the pyridine, (ν_d^{pyr}). We have also analyzed the changes of the IR bands upon complex formation associated with the four equivalent vibrational modes of the complexes **pyr**:C_6F_5Br and **pyr**:C_6F_5Cl (Fig. S4 and S5, ESI†).

The mode ν_a^{int} is only present in the complex and arises due to the halogen bonding. Therefore, we will first focus our analysis on the physical origin of ΔI for this peak. For ν_b^{C-X}, $\nu_c^{C_6F_5I}$ and ν_d^{pyr}, the frequency shifts upon complex formation are very small, which according to eqn (2) permits the direct decomposition of IR intensity changes. We note that the displacements of the two first modes include large variations of the halogen-bond distance, which is not the case for the latter two. Thus, ν_a^{int} and ν_b^{C-X} have a direct effect on the intermolecular interaction, in contrast with $\nu_c^{C_6F_5I}$ and ν_d^{pyr}. Even though the observed vibrational frequency shifts upon complex formation observed for modes localized on C_6F_5X (ν_b^{C-X}, $\nu_c^{C_6F_5I}$) are much smaller than that for mode ν_a^{int}, in all three cases we found a strong linear correlation between $\Delta\bar{\nu}$ and intermolecular interaction energy terms (see Table S4, ESI†).

Fig. 2b shows the partition of ΔI_a for the intermolecular vibrational stretching mode ν_a^{int} of the three **pyr**:C_6F_5X complexes ordered according to increasing values of the total interaction energy (see also Tables S5–S7, ESI†). Similarly to the pattern found for the interaction energy, the largest IR intensity changes are found for the complex with X = I and they decrease with increasing electronegativity of the halogen atom X. Indeed, as shown in Table S8 (ESI†), for this normal mode a good linear correlation with a very small y-intercept exists between the computed values of ΔE and ΔI_a for the three complexes ($R^2 = 0.93$). Also, mimicking the decomposition of ΔE, the partitioning of the intensity of the band associated to ν_a^{int} of **pyr**:C_6F_5I reveals that the increment of ΔI_a is mainly due to the sum of electrostatic and delocalization terms partially canceled by a large negative Pauli exchange-repulsion contribution. But now the total ΔI_a value is fairly well

This journal is © the Owner Societies 2023

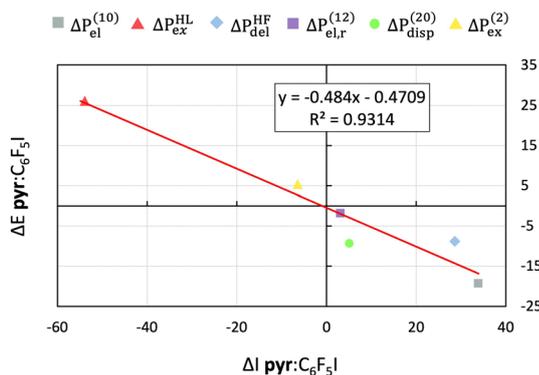*Phys. Chem. Chem. Phys.*, 2023, **25**, 20173–20177 | **20175**

Fig. 4 Linear fits between interaction-type contributions for the interaction energy ($\Delta P = \Delta E$) and the corresponding terms of the excess IR intensity ($\Delta P = \Delta I$) for ν_a^{int} for the **pyr**:C_6F_5I complex. Energies are given in kcal mol^{-1} and intensities in km mol^{-1}.

(up to $\approx$ 80%) described at the HF level. Nevertheless, as for ΔE, the electron correlation terms, especially the dispersion and second-order exchange contributions, also play an important role in ΔI_a of this normal mode. However, we should point out that the relative weight of the dispersion contribution decreases when the electronegativity of the halogen increases, again in agreement with the interaction energies.

Fig. 4 and Fig. S6, S7 (ESI†) show that for ν_a^{int} there is indeed a nice linear correlation with a small y-intercept between the values of the terms of the ΔE decomposition and those of the ΔI_a decomposition (*i.e.* $R^2 > 0.89$), indicating that both excess properties have the same physical nature in the sense defined above. The goodness-of-fit improves with the strength of the intermolecular interaction, giving the best linear correlation for the **pyr**:C_6F_5I complex. Similar good linear fits between the decomposition terms of the ΔE and ΔI are observed for the ν_b^{C-X} band of **pyr**:C_6F_5Br and **pyr**:C_6F_5I (see Table S8 and Fig. S8–S10, ESI†). On the contrary, we do not find a good linear correlation for **pyr**:C_6F_5Cl, possibly due to the strong deviation of the C–X–N angle from 180 (161), which reduces the coupling of ν_b^{C-X} vibration with the halogen bond distance. $\nu_c^{C_6F_5X}$ and ν_d^{pyr} bands also show a high linear correlation between the values of ΔE and ΔI. However, the decomposition of ΔI for those normal modes, which do not affect the halogen-bond distance, is very different from the decomposition of ΔI for ν_a^{int} and ν_b^{C-X}. For $\nu_c^{C_6F_5X}$ and ν_d^{pyr}, the relative weights and even the signs of the terms of ΔI change depending on the complex and normal mode (Tables S5–S7 and Fig. S11, ESI†). For instance, the largest contribution for $\nu_c^{C_6F_5Cl}$, $\nu_c^{C_6F_5Br}$, and $\nu_c^{C_6F_5I}$ is $\Delta I_{el}^{(10)}$, ΔI_{ex}^{HL} and ΔI_{del}^{HF}, respectively. Therefore, while for those vibrational modes that induce large variations of the halogen-bond distance the partitions of ΔI are strongly correlated with their ΔE counterparts, no such correlation is found for the other vibrational modes studied here.

To investigate if this observation can be generalized to other molecular complexes, the decompositions of ΔE and ΔI for three vibrational modes of two small halogen-bonded complexes (HCN:IF and HCN:BrF) and of three small hydrogen-bonded systems (HCN:HCl, HCN:HNC and HCN:HCN) were analyzed

(Fig. S12–S16 and Tables S9–S14, ESI†). As summarized in Table S15 (ESI†), for the intermolecular stretching of the five complexes the decomposition terms of ΔI are linearly correlated with the decomposition terms of ΔE ($R^2 > 0.83$). On the other hand, for the local vibrational modes the analogous linear correlation is usually not found, (*i.e.* the coefficients of determination (R^2) are between 0.20 and 0.80).

In summary, thanks to our recent development of a new computational scheme to decompose the IR spectra of molecular complexes in terms of intermolecular interaction energy components, we have shown for different types of systems and intermolecular bonds that the partitions of ΔE and ΔI are strongly linearly correlated, with a very small y-intercept, for the vibrational modes which involve substantial variations of the intermolecular bond length. Therefore, for such modes, the physical origin of the changes in the corresponding IR bands in terms of interaction types is similar to the interaction energy, which implies that both excess properties have equivalent physical nature. This is not true for other vibrational modes localized in one of the monomers studied here, for which the corresponding interaction-induced changes in IR bands may present a completely different decomposition than the interaction energy.

Conflicts of interest

There are no conflicts to declare.

Acknowledgements

References

1 K. Morokuma, *J. Chem. Phys.*, 1971, **55**, 1236–1244.
2 T. Ziegler and A. Rauk, *Theor. Chim. Acta*, 1977, **46**, 1–10.
3 K. Kitaura and K. Morokuma, *Int. J. Quantum Chem.*, 1976, **10**, 325–340.
4 P. S. Bagus, K. Hermann and C. W. Bauschlicher, *J. Chem. Phys.*, 1984, **80**, 4378.
5 W. J. Stevens and W. H. Fink, *Chem. Phys. Lett.*, 1987, **139**, 15–22.
6 E. D. Glendening and A. Streitwieser, *J. Chem. Phys.*, 1994, **100**, 2900.
7 Y. Mo, J. Gao and S. D. Peyerimhoff, *J. Chem. Phys.*, 2000, **112**, 5530.
8 P. Su and H. Li, *J. Chem. Phys.*, 2009, **131**, 014102.

9 P. R. Horn and M. Head-Gordon, *Phys. Chem. Chem. Phys.*, 2016, **18**, 23067.

10 A. Aldossary, M. Gimferrer, Y. Mao, A. K. D. Honxia Hao, P. Salvador, T. Head-Gordon and M. Head-Gordon, *J. Phys. Chem. A*, 2023, **127**, 1760–1774.

11 A. Buckingham, J. Del Bene and S. McDowell, *Chem. Phys. Lett.*, 2008, **463**, 1–10.

12 T. Fornaro, D. Burini, M. Biczysko and V. Barone, *J. Phys. Chem. A*, 2015, **119**, 4224–4236.

13 E. Arunan, G. R. Desiraju, R. A. Klein, J. Sadlej, S. Scheiner, I. Alkorta, D. C. Clary, R. H. Crabtree, J. J. Dannenberg, P. Hobza, H. G. Kjaergaard, A. C. Legon, B. Mennucci and D. J. Nesbitt, *Pure Appl. Chem.*, 2011, **83**, 1637–1641.

14 G. R. Desiraju, P. S. Ho, L. Kloo, A. C. Legon, R. Marquardt, P. Metrangolo, P. Politzer, G. Resnati and K. Rissanen, *Pure Appl. Chem.*, 2013, **85**, 1711–1713.

15 Q. Zhang, M. Chen, M. Zhou, D. M. Andrada and G. Frenking, *J. Phys. Chem. A*, 2015, **119**, 2543–2552.

16 D. Ojha, K. Karhan and T. Kühne, *Sci. Rep.*, 2018, **8**, 2045–2322.

17 A. Iglesias-Reguant, H. Reis, M. Medved, J. M. Luis and R. Zalesny, *Phys. Chem. Chem. Phys.*, 2023, **25**, 11658–11664.

18 A. Iglesias-Reguant, J. Zielak-Milewska, T. Misiaszek, R. Zalesny, J. M. Luis and B. Osmialowski, *J. Org. Chem.*, 2022, **87**, 15159–15165.

19 V. Vasylyeva, L. Catalano, C. Nervi, R. Gobetto, P. Metrangolo and G. Resnati, *CrystEngComm*, 2016, **18**, 2247–2250.

20 F. Meyer and P. Dubois, *CrystEngComm*, 2013, **15**, 3058–3071.

21 G. R. Desiraju, *J. Am. Chem. Soc.*, 2013, **135**, 9952–9967.

22 W. Wang, Y. Zhang and W. J. Jin, *Coord. Chem. Rev.*, 2020, **404**, 213107.

23 J. K. Salunke, N. A. Durandin, T.-P. Ruoko, N. R. Candeias, P. Vivo, E. Vuorimaa-Laukkanen, T. Laaksonen and A. Priimagi, *Sci. Rep.*, 2018, **8**, 14431.

24 K. M. Bak, S. C. Patrick, X. Li, P. D. Beer and J. J. Davis, *Angew. Chem., Int. Ed.*, 2023, **62**, e202300867.

25 P. Auffinger, F. A. Hays, E. Westhof and P. S. Ho, *Proc. Natl. Acad. Sci. U. S. A.*, 2004, **101**, 16789–16794.

26 R. Wilcken, M. O. Zimmermann, A. Lange, A. C. Joerger and F. M. Boeckler, *J. Med. Chem.*, 2013, **56**, 1363–1388.

27 W.-S. Zou, S. Lin, J.-Y. Li, H.-Q. Wei, X.-Q. Zhang, D.-X. Shen, J.-Q. Qiao, H.-Z. Lian, D.-Q. Xie and X. Ge, *New J. Chem.*, 2015, **39**, 262–272.

28 T. Clark, M. Hennemann and J. Murray, *et al.*, *J. Mol. Model.*, 2007, **13**, 291–296.

29 B. Mallada, A. Gallardo, M. Lamanec, B. de la Torre, V. Spirko, P. Hobza and P. Jelinek, *Science*, 2021, **374**, 863–867.

30 S. Yu, J. S. Ward, K.-N. Truong and K. Rissanen, *Angew. Chem., Int. Ed.*, 2021, **60**, 20739–20743.

31 N. Bedekovic, L. Fotovic, V. Stilinovic and D. Cincic, *Cryst. Growth Des.*, 2022, **22**, 987–992.

32 M. Gutowski, F. V. Duijneveldt, G. Chałasiński and L. Piela, *Mol. Phys.*, 1987, **61**, 233–247.

33 W. A. Sokalski, S. Roszak and K. Pecul, *Chem. Phys. Lett.*, 1988, **153**, 153–159.

34 S. M. Cybulski, G. Chałasiński and R. Moszyński, *J. Chem. Phys.*, 1990, **92**, 4357–4363.

35 G. Chałasiński and M. M. Szcześniak, *Chem. Rev.*, 1994, **94**, 1723–1765.

36 G. Chałasiński and M. M. Szcześniak, *Mol. Phys.*, 1988, **63**, 205–224.

37 F. B. van Duijneveldt, J. G. C. M. van Duijneveldt-van de Rijdt and J. H. Van Lenthe, *Chem. Rev.*, 1994, **94**, 1873–1885.

38 R. Moszyński, S. Rybak, S. Cybulski and G. Chałasiński, *Chem. Phys. Lett.*, 1990, **166**, 609–614.

39 M. Medved, A. Iglesias, H. Reis, R. Góra, J. M. Luis and R. Zaleśny, *Phys. Chem. Chem. Phys.*, 2020, **22**, 4225–4234.

This journal is © the Owner Societies 2023

Phys. Chem. Chem. Phys., 2023, **25**, 20173–20177 | **20177**